CHAPTER 5

RESULTS AND DISCUSSION: PHOSPHATE REMOVAL BY FLY ASH

5.1. Particle dimensions and chemical composition

Figure 5.1 shows the particle size distribution for the fly ash, obtained by Fraunhofer diffraction particle analysis as described in Experimental Section 4.3.1.

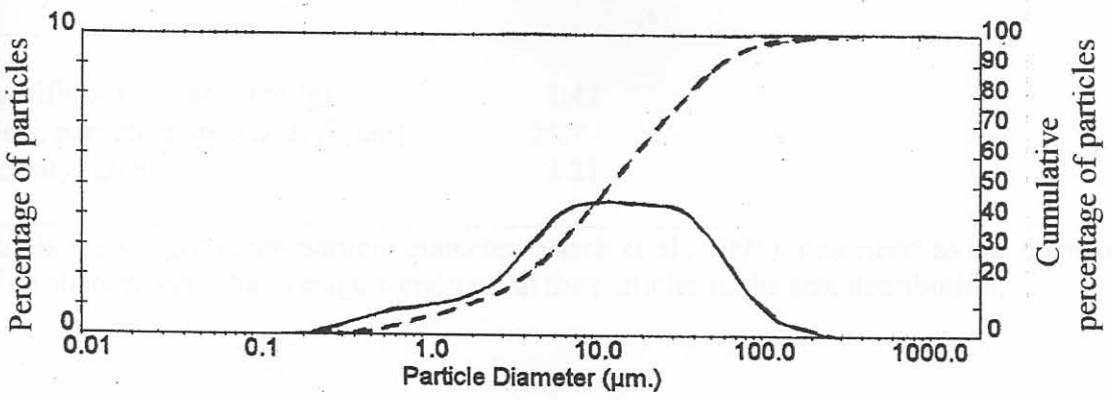

Figure 5.1. Particle size distribution for the FA sample.

The solid line represents the percentage of particles having a given diameter, the particle size distribution being a logarithmic function of the individual particle sizes (see equation (3.1)). The existence of the plateau indicates a slight deviation from a log-normal curve; this was probably influenced by factors such as the origin of the coal and the burning conditions in the boiler.

The broken line is a cumulative curve that represents the percentage of particles whose diameters are less than a given diameter. About 63 % of the particles were found to have diameters in the 5-50 μm size range.

Some important physical properties are summarised in Table 5.1.

Table 5.1. Physical properties of FA.

Characteristic	Value
Specific surface area (m^2/g)	1.42
Mean particle diameter $d_{4,3}$[a] (μm)	25.7
Density (g/cm^3)	2.21

[a] $d_{4,3}$ is the weight mean particle diameter (Black et al., 1996), described as the diameter of a sphere having the average weight of all the particles in the size distribution.

Figure 5.2 shows the XRD data accumulated over the 5-80° 2θ range. Fly ash typically contains over 50 % glass, which usually contains aluminium and silica. The glass hump can be seen clearly at ca 25° 2θ. The high background is due to the amorphous nature of the sample, i.e. mineral matter in the form of glassy particles.

Although the background was high, peaks for mullite ($Al_6Si_2O_{13}$) and quartz (SiO_2) (typical fly ash crystalline phases) were discernible in the diffractogram even without prior smoothing and background correction.

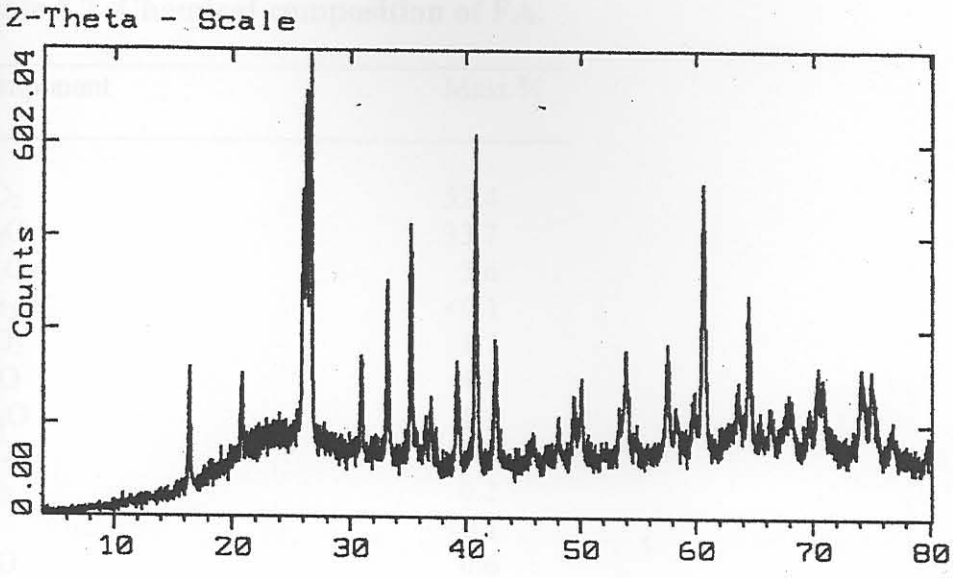

Figure 5.2. Diffractogram of the FA sample.

Characteristic peaks for mullite were identified at ca 16.5, 26.2, 35.3, 41, 60.5 and 64.5° 2θ. Quartz peaks were identified at ca 21, 26.5 and 50 2θ. Sillimanite (Al_2SiO_5), a member of the mullite family with less alumina, also appears to be present with peaks identified at 26 and 37.1° 2θ.

The chemical oxide composition obtained by XRF is shown in Table 5.2. The relatively low CaO content (4.1 %) typifies the Matla fly ash sample as a Class F fly ash.

Table 5.2. Chemical composition of FA.

Component	Mass %
SiO_2	52.4
Al_2O_3	33.7
Fe_2O_3	3.6
Mn_2O_3	<0.1
TiO_2	1.7
CaO	4.1
MgO	1.1
P_2O_5	0.3
SO_3	0.2
Cl	<0.1
K_2O	0.6
Na_2O	0.5
LOI @ 1000°C	0.8
Total	99.0

5.2. Calibration curve for UV/VIS analysis of PO_4^{3-} in aqueous solution

The calibration curve obtained is shown in Figure 5.3. Curvilinear regression (Miller and Miller, 1993) established the upper limit of linearity to be ca 55 mg/l PO_4^{3-} (as P), with a detection limit (3σ) of 0.2 mg/l and regression equation

$$y = 0.002948 + 0.01842\,x$$

over the linear range (R^2= 0.9998), between $0 < [PO_4^{3-}] < 50$ mg/l.

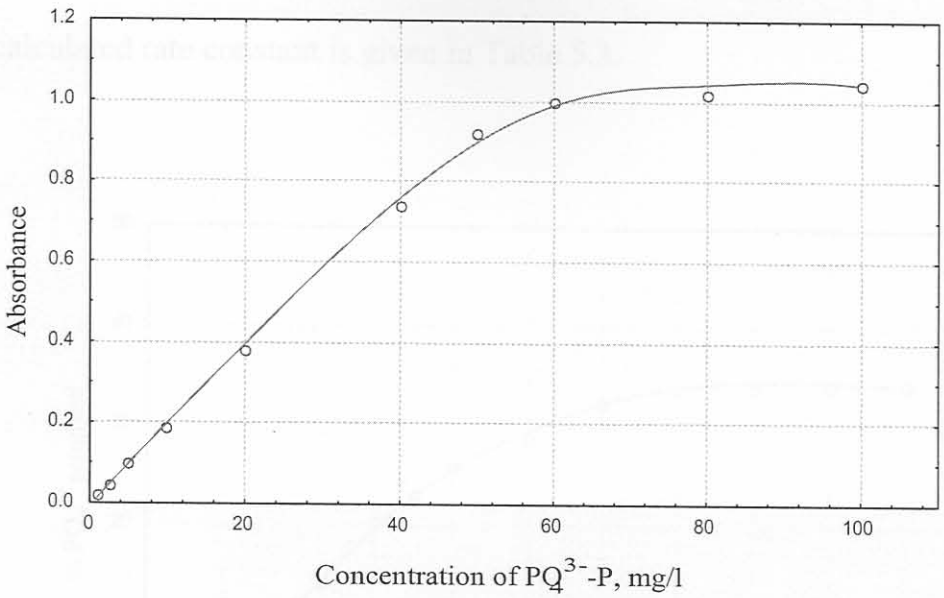

Figure 5.3. UV/VIS analysis calibration curve for PO_4^{3-}.

5.3. Kinetics

Figure 5.4 illustrates the percentage PO_4^{3-} removed with time, measured as described in Experimental Section 4.3.4. It can be seen that the uptake of PO_4^{3-} virtually ceased after a contact time of about 6 hrs; this is indicative of the onset of dynamic equilibrium.

The fractional attainment of equilibrium as a function of time, assuming a first order reversible kinetics model, is given by equation (1.12) as explained in Section 1.3. A plot according to equation (1.12) is shown in Figure 5.5. The good straight-line fit observed (linear correlation coefficient R^2= 0.991) indicates that the

sorption reaction may be approximated by first order reversible kinetics. The calculated rate constant is given in Table 5.3.

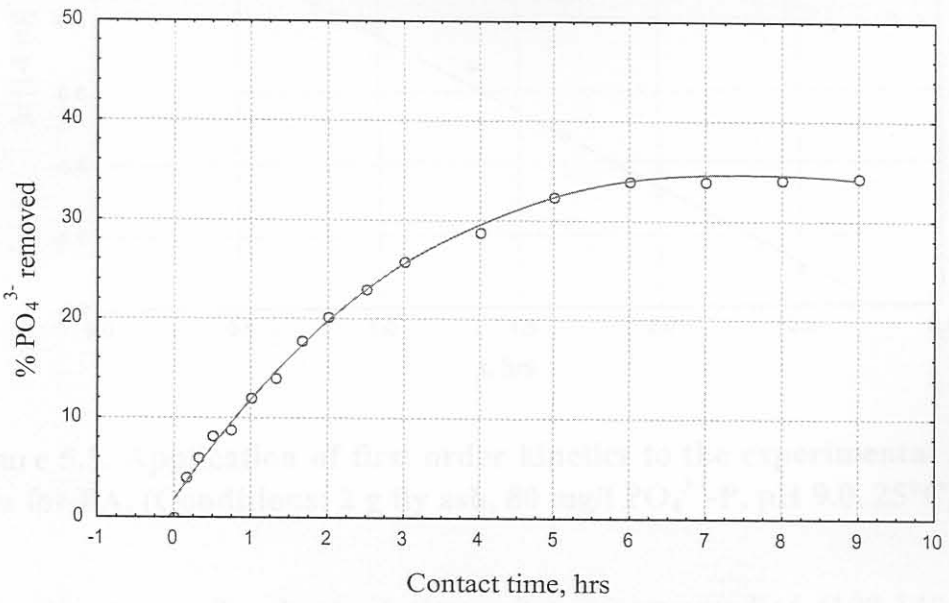

Figure 5.4. Kinetics of PO_4^{3-} removal by FA.
(Conditions: 2 g FA, 80 mg/l PO_4^{3-}-P, pH 9.0, 25°C)

Table 5.3. Values of first order reaction rate constant and intra-particle diffusion constant for PO_4^{3-} removal by FA.

Parameter	Value
k' (per hour)	0.423
D (cm^2/s)	8.40×10^{-12}

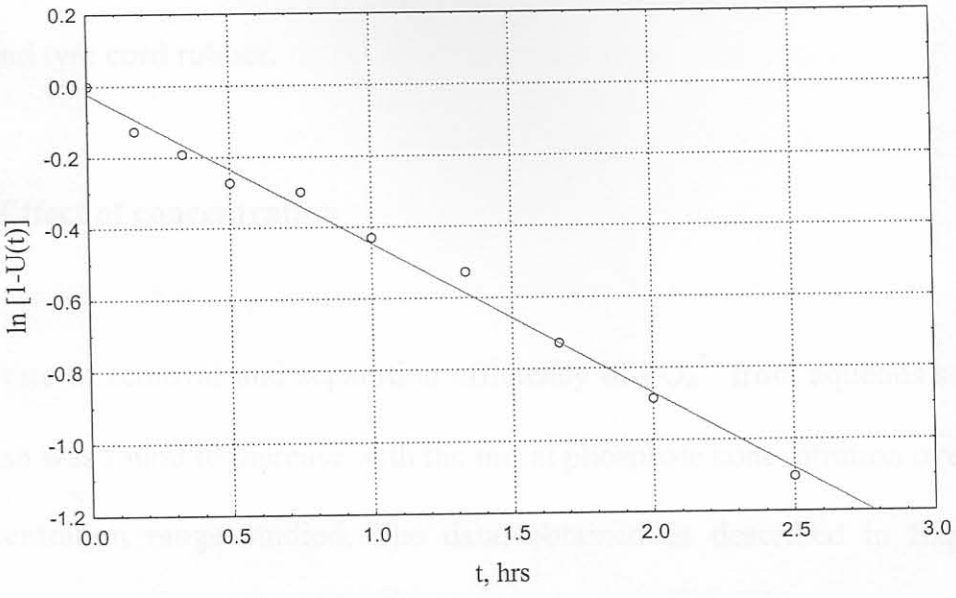

Figure 5.5. Application of first order kinetics to the experimental adsorption data for FA. (Conditions: 2 g fly ash, 80 mg/l PO_4^{3-}-P, pH 9.0, 25°C)

Over the range of sorbent-solution agitation rates studied (100-140 cycles per minute horizontally) it was observed that the sorption rate was not affected by the rate of mixing. This suggests that diffusion in the pores of sorbent particles rather than diffusion through the film at the sorbent particle-aqueous solution interface is rate limiting, which would provide evidence that intra-particle diffusion is the controlling resistance rather than external diffusion.

The value of the intra-particle diffusion constant D calculated using equation (1.13) is given in Table 5.3. According to Michelsen et al. (1975), the value of D should be in the range 10^{-11}-10^{-13} cm^2/s for pore diffusion to be rate limiting; although it must be pointed out immediately that the system they studied involved

the removal of heavy metals such as Hg using ion-exchange products made from ground tyre cord rubber.

5.4. Effect of concentration

The rate of removal and separation efficiency of PO_4^{3-} from aqueous solution by fly ash was found to increase with the initial phosphate concentration over the concentration range studied. The data, obtained as described in Experimental Section 4.3.5.1, is represented in Figure 5.6.

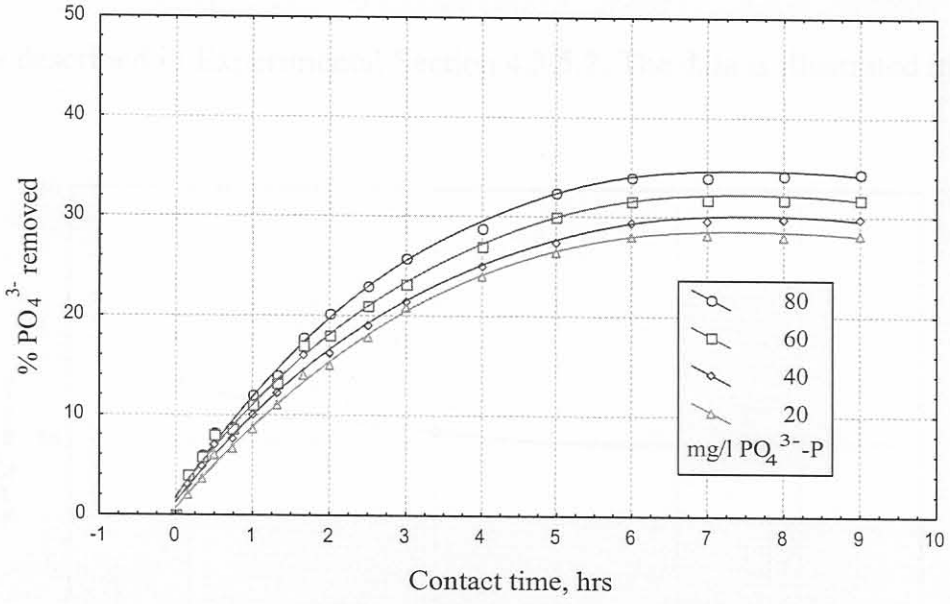

Figure 5.6. Effect of concentration on the kinetics of PO_4^{3-} removal by FA. (Conditions: 2 g FA, pH 9.0, 25°C)

The observed increase in the percentage PO_4^{3-} removed with increasing solute concentration (for the same amount of sorbent) is hardly surprising if the system

under study is non-ideal. As mentioned in Sections 1.2.1 and 1.2.2, for non-ideal systems the mass of solute adsorbed per mass of sorbent keeps increasing as the concentration of the solute increases. This has been ascribed to surface heterogeneity in such systems. Interestingly, the initial phosphate concentration does not appear to influence the time it takes (ca 6 hrs) for PO_4^{3-} removal to reach equilibrium.

5.5. Effect of particle size

The effect of sorbent particle size on the percentage PO_4^{3-} removed was measured as described in Experimental Section 4.3.5.2. The data is illustrated in Figure 5.7.

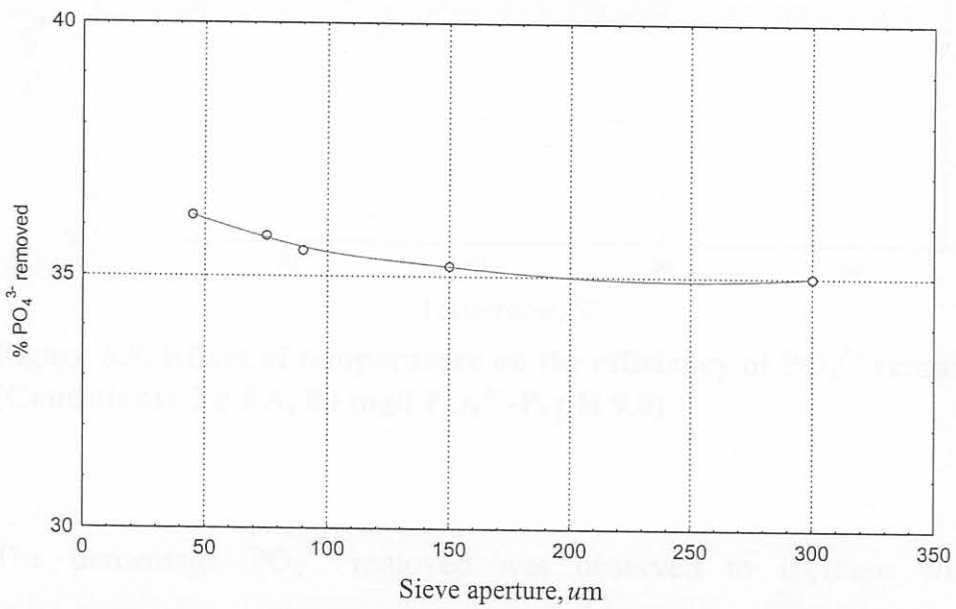

Figure 5.7. Effect of particle size on the efficiency of PO_4^{3-} removal by FA. (Conditions: 2 g fly ash, 80 mg/l PO_4^{3-}-P, pH 9.0, 25°C)

Although there was some increase in the percentage PO_4^{3-} removed as the particle size decreased, this increase does not appear to be proportional to the increased surface area.

5.6. Effect of temperature

The effect of temperature on the percentage PO_4^{3-} removed was measured as described in Experimental Section 4.3.5.3. The data is illustrated in Figure 5.8.

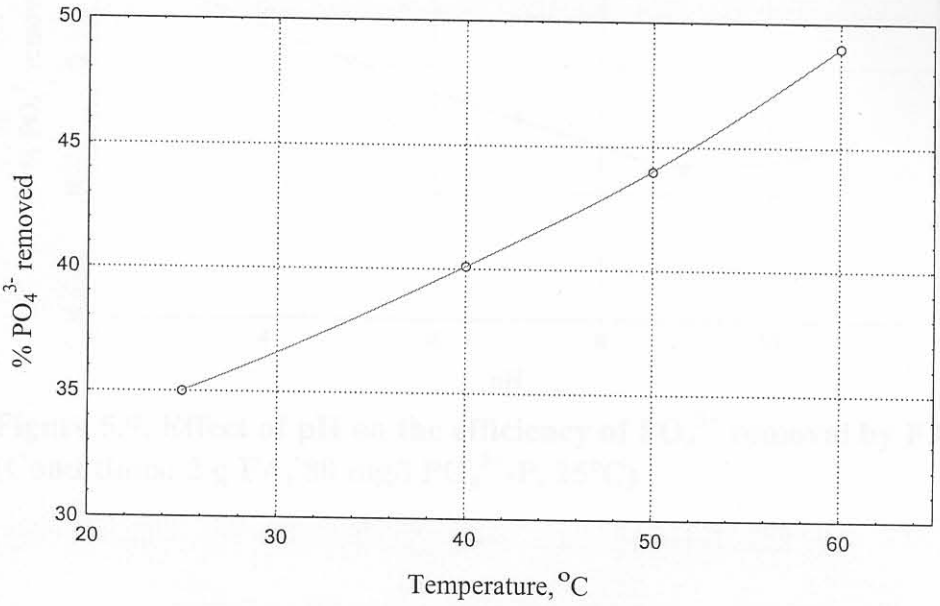

Figure 5.8. Effect of temperature on the efficiency of PO_4^{3-} removal by FA. (Conditions: 2 g FA, 80 mg/l PO_4^{3-}-P, pH 9.0)

The percentage PO_4^{3-} removed was observed to increase with increasing temperature. This is probably due to the resulting increase in diffusion rate.

5.7. Effect of pH

The variation of the percentage PO_4^{3-} removed with the initial pH of the aqueous solution was measured as described in Experimental Section 4.3.5.4. The data obtained is shown in Figure 5.9.

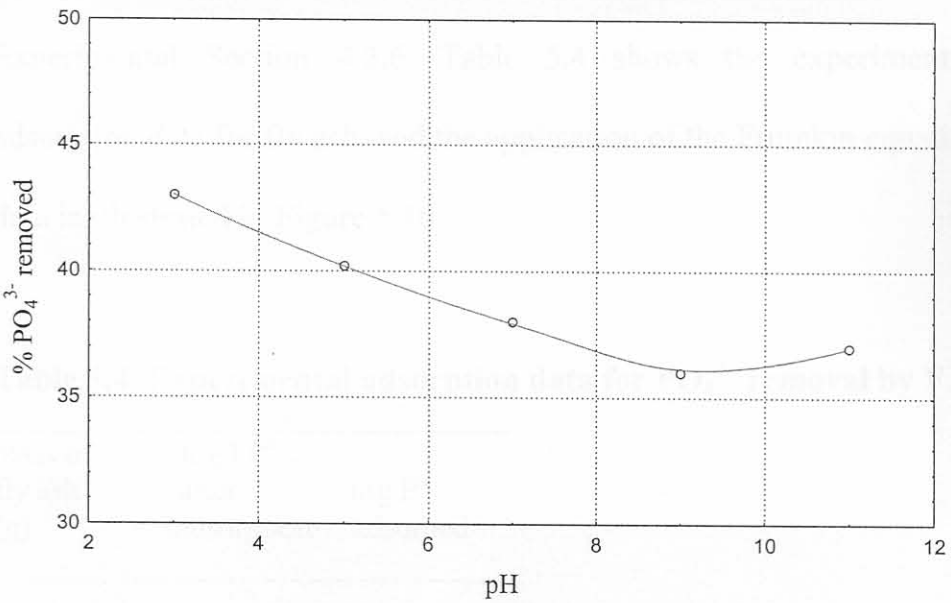

Figure 5.9. Effect of pH on the efficiency of PO_4^{3-} removal by FA. (Conditions: 2 g FA, 80 mg/l PO_4^{3-}-P, 25°C)

It can be seen from the figure that the efficiency of PO_4^{3-} removal increases steadily in acidic pH. This may be due to the accumulation of positive charge on the adsorbent surface that increases its affinity for the negatively charged phosphate ions. The observed slight increase in the efficiency of PO_4^{3-} removal beyond pH 9 could be due to the creation of favourable conditions for calcium

phosphate precipitation at high pH, thus enhancing the removal of PO_4^{3-} by some dissolved calcium present in the fly ash.

5.8. Adsorption isotherms

Adsorption data for modelling adsorption isotherms was obtained as described in Experimental Section 4.3.6. Table 5.4 shows the experimentally obtained adsorption data for fly ash, and the application of the Frumkin equation (1.7) to the data is illustrated in Figure 5.10.

Table 5.4. Experimental adsorption data for PO_4^{3-} removal by FA.

mass of fly ash (g)	mg/l P[a] after adsorption	mg P[a] adsorbed
0.5	72.8	5.4
2	71.9	5.6
3	71.4	5.7
3.5	70.2	6.4
4	65.0	7.0
5	58.7	8.3

[a] PO_4^{3-} (as P)

Attempts to fit the data to the Langmuir (equation 1.3) and Freundlich (equation 1.4) isotherms yielded non-linear plots with values of $R^2 < 0.4$. It is evident that the

Frumkin isotherm (see equations 1.6 & 1.7) is the appropriate one for fitting the data, which is indicative of a non-ideal system with finite lateral interactions among adsorbate particles. The Frumkin constants were calculated and are shown in Table 5.5.

Table 5.5. Isotherm linear correlation coefficients and Frumkin constants for PO_4^{3-} adsorption by FA.

Isotherm	R^2	α	β
Frumkin	0.992	3.061	0.025
Langmuir	0.376		
Freundlich	0.279		

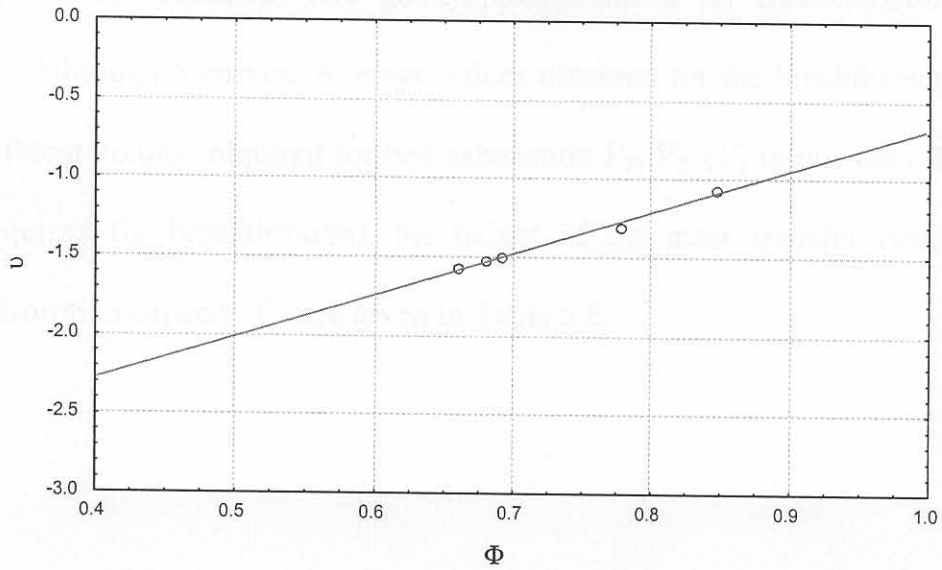

Figure 5.10. Application of the Frumkin equation to the experimental adsorption data (given in Table 5.4) for FA.

5.9. Breakthrough curves

Data for constructing breakthrough curves was obtained as described in Experimental Section 4.3.7. The data obtained for the breakthrough experiments (see equations 1.15 and 1.16) for fly ash are shown in Table 5.6, and a representative breakthrough curve is illustrated in Figure 5.11.

Table 5.6. Breakthrough data for FA.

t_E (min)	V_T (cm^3)	V_Z (cm^3)	h_Z (cm)	C_T (mg PO_4^{3-}-P/g)
2.8	187	116	1.742	32

The curves obtained were good approximations for characteristic symmetrical breakthrough S curves. Average values obtained for the breakthrough time t_E, the effluent volume required for bed exhaustion V_T, V_Z (V_T minus the effluent volume required for breakthrough), the height of the mass transfer zone h_Z, and the adsorption capacity C_T are given in Table 5.6.

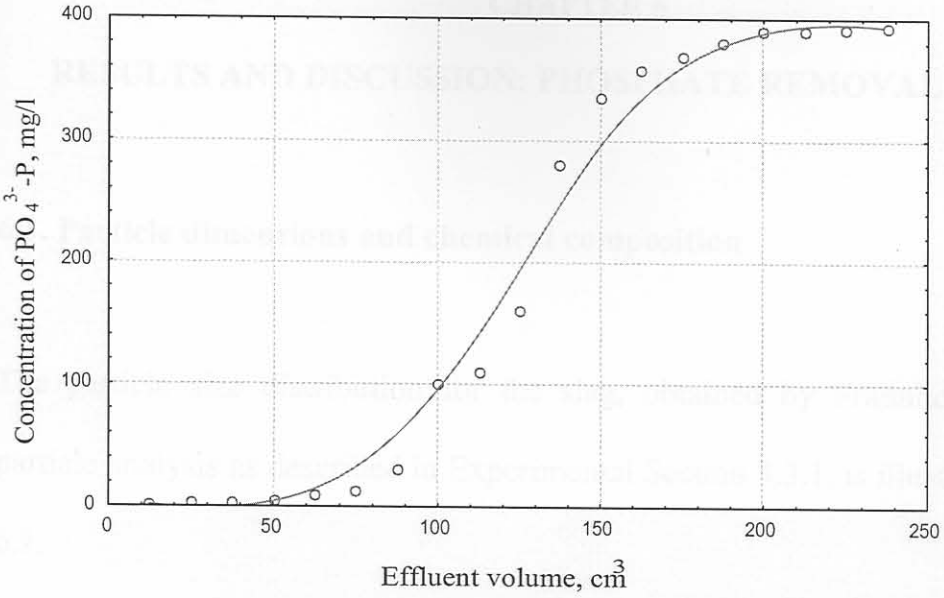

Figure 5.11. Breakthrough curve for PO_4^{3-} removal by FA.

An average C_T value of 32 mg PO_4^{3-}-P/g was obtained for fly ash.